forests

MDPI

Article

Single-Step GWAS Multi-Trait Threshold Linear Model for Growth Rate and Heteroblasty in *Eucalyptus globulus*

Milena Gonzalez [1,*], Ignacio Aguilar [2], Marianella Quezada [3] and Gustavo Balmelli [1]

[1] Instituto Nacional de Investigación Agropecuaria (INIA), Tacuarembó 45000, Uruguay; gbalmelli@inia.org.uy
[2] Instituto Nacional de Investigación Agropecuaria (INIA), Montevideo 11500, Uruguay; iaguilar@inia.org.uy
[3] Departamento de Biología Vegetal, Facultad de Agronomía, Universidad de la República, Montevideo 12900, Uruguay; mquezada@fagro.edu.uy
* Correspondence: mileg2014@gmail.com

Abstract: *Eucalyptus globulus* Labill. is one of the most important species in the paper industry. *Teratosphaeria nubilosa* has affected plantations worldwide, infecting young foliage. Genome-wide association studies (GWASs) are essential to identify genomic segments associated with susceptibility to this disease. The inclusion of genomic strategies in breeding programs is key to the sustainability of the species. The aim of this study was to identify genomic regions associated with growth and heteroblasty (change from juvenile to adult foliage: ADFO) in a tree breeding population of *E. globulus*. Tree growth was measured as total height (TH) and diameter at breast height (DBH). All traits were evaluated at 14 and 21 months. A multi-trait threshold linear model was developed following the single-step genomic selection methodology. Genetic correlations (r_g) and narrow-sense heritability (h^2) for all traits were estimated. Windows of 0.2 Mb were used. Only the windows with an estimated variance greater than 1% were considered. The r_g ranged from 0.51 to 0.97. The h^2 was high for ADFO (0.83–0.84) and lower for HT (0.37) and DBH (0.53). In growth traits, no QTLs were found that explained more than 1% of the variance. However, two genomic regions related to ADFO were identified on chromosomes 3 and 11.

Keywords: GWAS; threshold linear model; QTLs; tree breeding

Academic Editor: David Lee

Received: 4 December 2024
Revised: 31 December 2024
Accepted: 8 January 2025
Published: 28 January 2025

Citation: Gonzalez, M.; Aguilar, I.; Quezada, M.; Balmelli, G. Single-Step GWAS Multi-Trait Threshold Linear Model for Growth Rate and Heteroblasty in *Eucalyptus globulus*. *Forests* **2025**, *16*, 247. https://doi.org/10.3390/f16020247

1. Introduction

Most agronomic traits of interest to breeders are quantitative and polygenic, controlled by numerous small-effect genes [1]. The first genome-wide association studies (GWASs) marked a significant advancement in genetics by enabling researchers to identify genetic variants associated with complex traits and diseases across the entire genome [2–4]. Subsequent studies demonstrated that multi-trait models enhance the power to detect QTLs, particularly for highly correlated traits [5–7]. Bolormaa et al. [8] reported in dairy cattle that the multivariate analyses uncovered SNP associations that were not discovered by univariate analyses and that the benefit of a multiple-trait analysis increased if the traits were highly correlated. Cappa et al. [7] showed in lodgepole pine that multi-trait GWASs provide a substantial increase in the number of significant SNP markers identified and in the potential for identifying pleiotropic effects of individual genes, confirming the statistical power of these models.

Many methods are being developed for GWASs, and a commonly used approach involves converting genomic breeding values from GBLUP into estimated marker effects through a linear transformation, as described by Gualdrón [9]. One limitation of this method is that it only incorporates phenotypes from genotyped individuals. Thus, GBLUP

methods were expanded to incorporate information from non-genotyped individuals in prediction analyses, a method known as single-step genomic best linear unbiased prediction (ssGBLUP) [10]. This methodology is based on an infinitesimal model, which assumes equal variance for all single-nucleotide polymorphism (SNP)-associated effects on quantitative trait loci (QTLs), resulting in an identical genomic relationship matrix for all traits within a population [11].

Several models are used to test the significance of single-nucleotide polymorphism (SNP) effects [12], such as EMMAX (Efficient Mixed-Model Association eXpedited). This method fits a mixed model to account for relatedness and population structure while testing SNP associations [13]. However, SNPs within a genomic segment can be highly correlated with each other and jointly influence the phenotype, which makes identifying the effect of a single SNP difficult [14]. Therefore, GWASs based on testing genomic windows have been proposed to overcome this problem using Bayesian approaches [15]. The advantages of using windows of consecutive SNPs are that they can capture the effect of a QTL better than a single SNP, particularly since SNPs may be in linkage disequilibrium (LD) with a QTL and are useful for discriminating important effects from statistical noise [16,17]. Several studies have used windows of different sizes [8,18], but the optimal window size may also depend on the effective population size [19].

In tree breeding, most GWAS models have been applied to quantitative traits, such as volume. Categorical traits like forkings, survival, and stem straightness are also analyzed as quantitative traits, with or without transformation [20]. However, due to the lack of specific analysis tools, methods designed for binary and quantitative traits have been used to analyze categorical data, which is inappropriate and can lead to erroneous results [21]. Wright [22] developed the threshold concept to map a normally distributed underlying variable to the observed ordered categorical phenotypes. Gianola and Foulley [23] developed the threshold mixed-effects model, which has become popular for pedigree-based genetic evaluation of ordinal categorical traits. Misztal et al. [24] stated that threshold models have been applied in animal breeding for traits with categorical data.

In several plants, including *Eucalyptus*, the adult foliage may exhibit increased resistance to foliar diseases caused by pathogens like *Mycosphaerella* and *Teratosphaeria* [25]. These pathogens predominantly infect juvenile and intermediate foliage, causing severe leaf spotting, necrosis, defoliation, and shoot blight [26]. This resistance is often due to age-related changes in leaf morphology, chemistry, and physiology, which make mature leaves less susceptible to infection [25–27]. The use of fungicides to control *Mycosphaerella* and *Teratosphaeria* is expensive and impractical [26]. The expression of genetic variation for disease resistance in field trials will be influenced by the type and severity of the disease infestation, and some studies suggest that foliar resistance is under relatively strong genetic control [27–29]. Understanding plant defense mechanisms could be the key to improving disease management strategies [30–32].

The aim of this study was to identify genomic regions associated with both quantitative traits (growth) and categorical traits (heteroblasty) using a multi-trait threshold linear model and the single-step GWAS methodology in a tree breeding population of *Eucalyptus globulus*.

2. Materials and Methods

2.1. Study Population

The study population belongs to the *Eucalyptus globulus* tree improvement program of INIA Uruguay. It consists of parent trees and six progeny trials. The parent trees come from two seed orchards that include the parents of the six progeny tests. These two seed orchards, which contain both selected and non-selected trees, were established in 1996 (first generation) and 2002 (second generation). The phenotypic data were collected

from progeny tests planted in typical *Eucalyptus globulus* plantation areas in southeastern Uruguay, specifically in the departments of Lavalleja and Rocha. The first progeny test consists of half-sib families, represented by 3853 individuals from 194 open-pollinated (OP) families, planted in 2011 (for more details, see Quezada et al. [33]). The remaining five progeny tests consist of full-sib families, represented by 6051 individuals from 137 controlled matings (CMs), planted between 2015 and 2019 (Table 1). The OP families mainly come from the first-generation seed orchard, while the CM families originate from the second-generation seed orchard.

Table 1. Summary of phenotypic and genotypic information per trial.

Trials	Installation Year	Matting Type	Number of Families	Number of Trees Phenotyped	Number of Trees Genotyped
Parents (seed orchard first generation)	1996	OP	109	604	80
Parents (seed orchard second generation)	2002	OP	76	455	446
Progeny test 1	2011	OP	194	3756	975
Progeny test 2	2014	CM	24	551	87
Progeny test 3	2015	CM	22	644	108
Progeny test 4	2016	CM	42	989	194
Progeny test 5	2017	CM	39	1591	199
Progeny test 6	2019	CM	66	2276	320
Total				10,373	2409

2.2. Phenotypic Information

Tree growth was measured as total height (TH) and diameter at breast height (DBH) at 14 and 21 months, respectively. The precocity of change from juvenile to adult foliage (ADFO) was also assessed at these ages. ADFO was calculated as the percentage of the crown covered by adult foliage, using a visual scale with percentage intervals of 10%. Since the distribution of data across the different categories was not uniform, the values were grouped into three categories for analysis: 1 = no adult foliage, 2 = up to 50% adult foliage, and 3 = more than 50% adult foliage. ADFO was considered a categorical trait, while TH and DBH were treated as quantitative traits. At 14 months, most individuals had only juvenile foliage. By 21 months, most individuals had up to 50% adult foliage. In both assessments, the proportion of individuals with more than 50% adult foliage was low (Figure 1).

2.3. Genotypic Information

The genotypic information consisted of a total of 2409 individuals, including parents and progeny (OP and CM) (Table 1). Genotyping was performed using the Eucalyptus EUchip60K SNP chip at GeneSeek Inc. (Lincoln, NE, USA) [34].

The marker data were filtered to select markers with a call rate >0.95 and a minor allele frequency (MAF) >0.05, and individuals with a call rate >0.80, using the PREGSF90 version 1.26 software [35]. After filtering, 15,821 effective markers and 2359 individuals were retained. Pedigree correction was conducted using the SeekParent version 1.56 program from the BLUPF90 family [36]. The SNP density plot was generated using the R package version 4.2.3 CMPlot [37].

To analyze the genetic diversity of the parents, half-sibs, and full-sibs, principal component analysis (PCA) was performed using PREGSF90 from the BLUPF90 family of programs [35]. The three different groups were represented by different colors using the ggplot2 [38] R package [39]. The PCA was based on the H matrix [40].

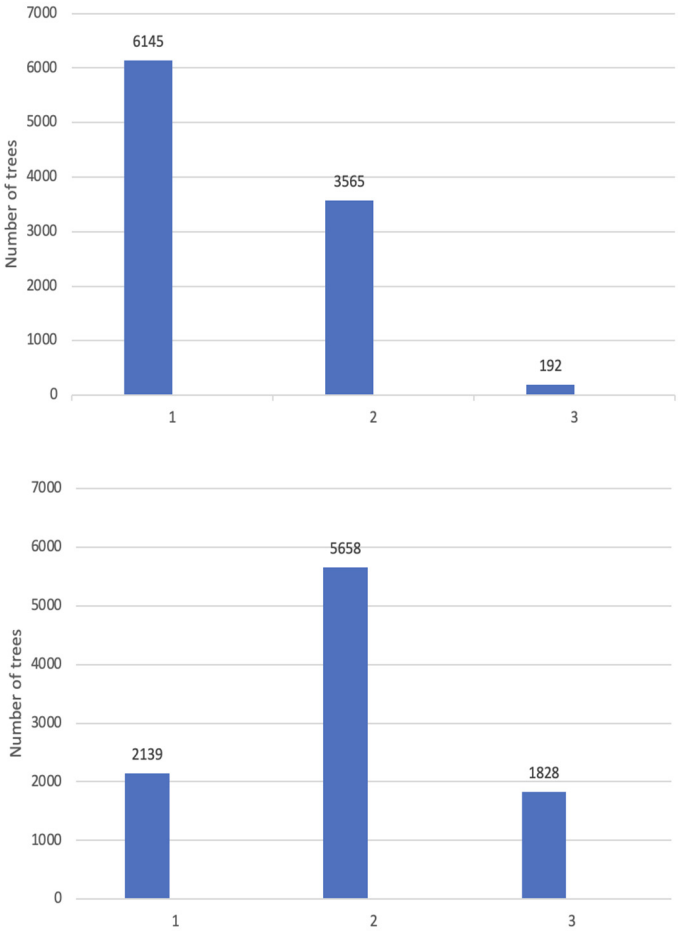

Figure 1. Frequency distribution for the different categories of adult foliage (ADFO) at 14 months (above) and at 21 months (below). 1 = no adult foliage, 2 = up to 50% adult foliage, and 3 = more than 50% adult foliage. The number above the bar corresponds to the number of trees.

2.4. Single-Step GWAS Model (ssGWAS)

A multi-trait threshold linear model was developed following the single-step genomic selection methodology [11], using a transformation of the genomic breeding values (a) to estimate SNP effects through equivalent models [41]. The multi-trait threshold linear ssGWAS model was estimated using variance and covariance matrices between the traits and residual errors, as specified by Equation (1):

$$y = Xb + Wp + Za + e \quad (1)$$

where y is the vector of phenotypes (TH, ADFO at 14 months, DBH, and ADFO at 21 months); b is the vector of fixed effects, including the overall mean of sites and blocks (within site), with incidence matrix X; p is the vector of random plot effects, with incidence matrix W; a is the vector of random genetic additive effects of the individual trees, with incidence matrix Z; and e is the vector of random residuals. The variance structure was defined to include additive genetic, plot, and residual variances for each trait, incorporating both pedigree and genomic information:

$$\text{Var} = \begin{bmatrix} p \\ a \\ e \end{bmatrix} + \begin{bmatrix} I \otimes P_0 & 0 & 0 \\ 0 & H \otimes G_0 & 0 \\ 0 & 0 & I \otimes R_0 \end{bmatrix}$$

where H is the numerator relationship matrix; G_0, P_0, and R_0 are 4 × 4 matrices of (co)variances for additive genetics, plot effects, and residual variances corresponding to each trait. I is the identity matrix and ⊗ = the direct matrix product. H is constructed by combining information from markers and pedigree information [40].

The inverse of the relationship matrix combining pedigree and genomic information (H^{-1}) was derived by Aguilar et al. [11], as defined by Equation (2):

$$H^{-1} = A^{-1} + \begin{bmatrix} 0 & 0 \\ 0 & G^{-1} - {A_{22}}^{-1} \end{bmatrix} \quad (2)$$

where A^{-1} and ${A_{22}}^{-1}$ are the inverse of the pedigree relationship matrices for all individuals and only for the genotyped individuals, respectively, and G^{-1} is estimated according VanRaden [42].

Variance components were estimated using GIBBSF90 version 3.2 [43]. For variance components, the Gibbs sampling process comprised 300,000 rounds and 1 every 50th sample was stored. After discarding the first 10,000 samples as burn-in, posterior means were calculated. The genetic correlations for all traits was estimated by Equation (3):

$$rg_{ij} = \frac{\sigma_{ij}^2}{\sqrt{\sigma_i^2 + \sigma_j^2}} \quad (3)$$

where σ_i^2 and σ_j^2 are the additive genetic variance for the traits.

The narrow-sense heritability for all traits was estimated by Equation (4):

$$h^2 = \frac{\sigma_a^2}{\sigma_a^2 + \sigma_p^2 + \sigma_e^2} \quad (4)$$

where σ_a^2 is the additive genetic variance, σ_p^2 is the plot variance, and σ_e^2 is the residual variance.

The SNP effects were estimated using Equation (5):

$$\hat{u} = F' \frac{1}{2pj(1-pj)} G^{-1} \hat{a}_{22} \quad (5)$$

where F is the matrix of gene content adjusted for the observed allele frequencies and p_j is the allele frequency of the ith SNP, G^{-1} is the inverse of the genomic relationship matrix, and $\hat{a}_{22}$ is the vector of genomic breeding values for genotyped individuals. The ssGWAS models were fitted with POSTGSF90 version 1.84 of BLUPF90 family software [44].

Genetic variance for the windows was computed following Peters et al. [18], where breeding values for each window were estimated and then the variance of these breeding values was calculated. The window size used in this study was 0.2 Mb, as the linkage disequilibrium (LD) for *E. globulus*, estimated previously by Quezada et al. [33], is approximately 0.2 Mb. Only the windows with an estimated variance greater than 1% were considered.

3. Results

3.1. Genomic Information

SNP markers were distributed across all 11 chromosomes, with the highest densities observed on chromosomes 3, 5, and 8, and the lowest on chromosomes 1, 4, 9, and 10 (Figure 2).

Figure 2. The distribution of filtered SNPs in 1 Mb windows across the *Eucalyptus grandis* genome. The *x*-axis represents the distance in Mb and the *y*-axis represents the chromosome number of *Eucalyptus* spp. The legend presents the marker density.

The PCA revealed the diversity and population structure present in the studied population (Figure 3). The first two principal components explained 19.5% and 6.8% of the total variation. Based on these components, the majority of trees are clustered into a single primary group, leading to a population with limited diversity, which is typical of many forest genetic improvement programs.

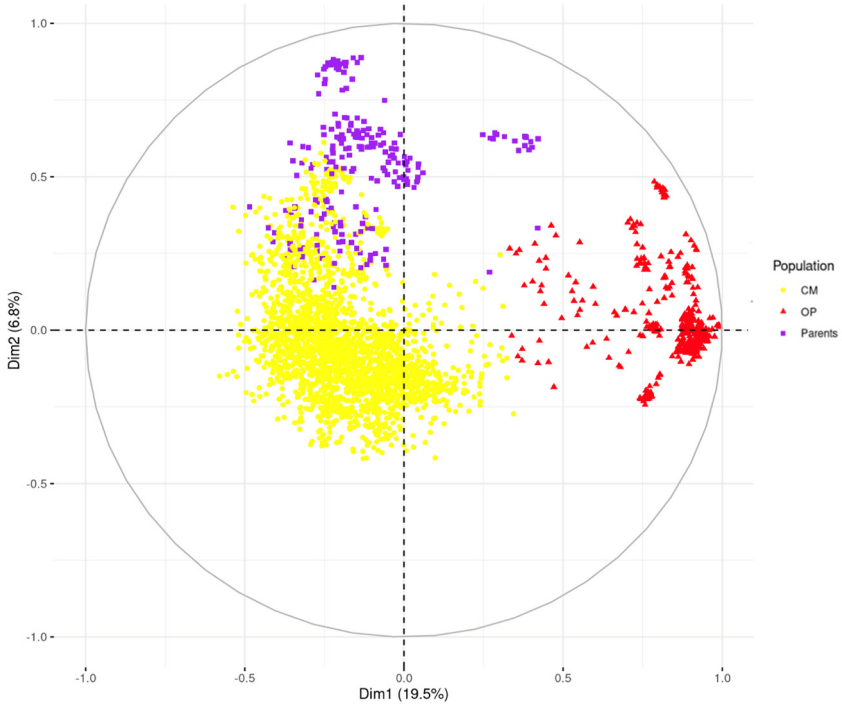

Figure 3. Principal component analysis for the parent population in violet (first- and second-generation seed orchard), half-sib first progeny test in red (OP), and full-sib progeny test 2 to 6 in yellow (CM).

3.2. Multi-Trait Threshold Linear ssGWAS Model

The genetic correlations for all traits were positive and ranged from moderate to high, with values ranging from 0.51 to 0.97 (Table 2). DBH exhibited the strongest correlation with all traits. The highest correlation was observed between ADFO at 14 and 21 months.

The heritabilities estimated were high for disease resistance traits (ADFO at 14 months and ADFO at 21 months) and lower for HT and DBH, with DBH showing a moderately higher heritability than HT. Heritability estimates ranged from 0.37 to 0.84.

Table 2. The genetic (r_g) correlations estimated (above diagonal) from the ssGWAS model for different traits in *Eucalyptus globulus* and narrow-sense heritability (diagonal), with the HPD (high posterior density) interval (95%) in parentheses.

	HT14	ADFO14	DBH21	ADFO21
HT14	0.37 (0.31–0.43)	0.52 (0.44–0.60)	0.83 (0.79–0.86)	0.51(0.44–0.59)
ADFO14		0.84 (0.79–0.89)	0.66 (0.60–0.72)	0.97 (0.95–0.98)
DBH21			0.53 (0.78–0.88)	0.70 (0.64–0.75)
ADFO21				0.83 (0.78–0.88)

The windows overlap with an average of 12 SNPs, ranging from 4 to 22 SNPs per 0.2 Mb window. The variance explained by the 0.2 Mb windows for the growth traits (TH and DBH) is less than 1.0%, with a homogeneous distribution across all chromosomes (Figure 4). The variance explained by the windows for ADFO14 and ADFO21 is greater than 1% in chromosomes 3 and 11, with chromosome 11 explaining up to 2.5% of the variance.

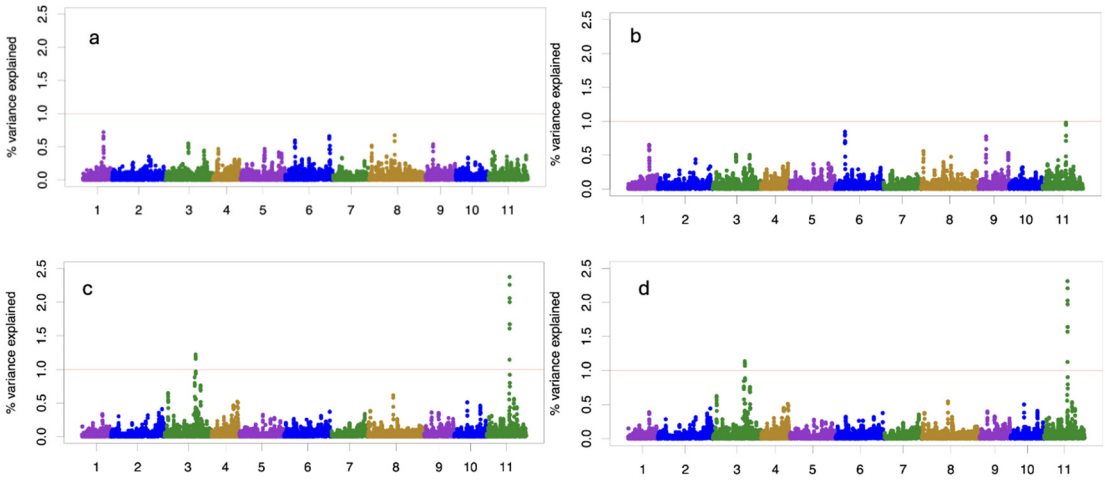

Figure 4. The variance explained by the 0.2 Mb windows of adjacent SNPs for TH at 14 months (**a**), DBH at 21 months (**b**), ADFO at 14 months (**c**), and ADFO at 21 months (**d**). The x-axis corresponds to the chromosome number of the species *E. globulus*, and each chromosome is represented with a different color. The y-axis corresponds to the total variance explained by the 0.2 Mb windows expressed as a percentage. The red line corresponds to the threshold considered to detect 0.2 Mb windows with a variance greater than 1%.

3.3. QTL Identifications

In the growth traits, no QTLs were found that explained more than 1% of the variance. However, two genomic regions (QTLs) were associated with the precocity of vegetative change (ADFO) measured at different ages (14 and 21 months). These genomic regions explained more than 1% of the total variance (Table 3). The QTLs were located on chromosomes 3 and 11, with 14 to 17 SNPs per 0.2 Mb window, respectively. Previous studies have linked these chromosomes to QTLs associated with disease resistance. These regions are crucial for understanding heteroblasty.

Table 3. Details of 0.2 Mb windows (QTL) that explained variance greater than 1% for proportion of adult foliage (ADFO) in *Eucalyptus globulus*.

Trait	Chr	N° SNPs	Start Position (Mb)	SNP Start	End Position (Mb)	SNP End	% Variance Explained
ADFO14 and ADFO21	3	14	49,472,132	EuBR03s49472132A4B0C0D30E1	49,646,842	EuBR03s49646842A4B1C0D60E1	1.22
ADFO14 and ADFO21	11	17	29,445,307	EuBR11s29445307A1B0C0D30E1	29,642,533	EuBR11s29642533A5B1C1D30E1	2.37

4. Discussion

In several countries, foliar diseases have caused devastating damage to young plantations of *E. globulus*, and the sustainability of this species depends on the rapid development of resistant genetic stock [27,45]. Some studies have focused on this issue, evaluating heteroblasty in tree species [33,46–48]. This study represents an additional step toward identifying genomic regions associated with complex traits, such as growth and scape to *T. nubilosa*, in *E. globulus*. Although the studied population lacks genetic diversity, significant associations between SNPs and phenotypes were identified. While less genetic variation is available in operational breeding populations, the associations found should be considerably more useful for informing practical breeding decisions [49,50]. In this work, we were able to evaluate the performance of a multi-trait threshold linear ssGWAS approach using windows in operational breeding populations.

The estimation of genetic parameters plays a crucial role in the management of seed orchards and provides valuable guidance for developing the evaluation and selection strategies for the next generation of improvement [51]. The strong genetic correlation (r_g = 0.97) between ADFO at 14 and 21 months suggests that early-stage evaluation at 14 months is a reliable predictor of later-stage traits, with ADFO at 14 months being a good indicator of ADFO at 21 months, thus reducing the time required for measurements. The estimated heritabilities for ADFO indicated strong genetic control, with values of 0.84 and 0.86 for ADFO14 and ADFO21, respectively. Furthermore, studies related to foliar diseases have reported lower heritabilities, ranging between 0.12 and 0.60 [28,33,52,53], but still confirm the strong genetic control of this trait, suggesting that the expected response to selection is relatively favorable. On the other hand, HT and DBH exhibited lower genetic control, with heritabilities of 0.37 and 0.53, respectively. These findings are consistent with previous works that reported similar heritabilities for HT and DBH in *Eucalyptus* spp., ranging from 0.13 to 0.44 [33,54–56].

The multi-trait threshold ssGWAS model was effective in identifying markers located in genomic regions that explained more than 1% of the variance for disease resistance traits (ADFO14 and ADFO21). Fernando et al. [57] affirm that most GWASs rely on inferences derived from joint tests on all SNP markers within a narrow genomic region, acknowledging that single SNP marker associations may suffer from low statistical power, multicollinearity issues, or both. Porter and O'Reilly [58] reported that multi-trait GWASs can be used to analyze multiple traits simultaneously and were specifically developed to enhance statistical power and identify pleiotropic loci. Additionally, Fernandes et al. [59] emphasize that multi-trait GWASs are a valuable addition to the array of statistical models commonly used to investigate the genetic architecture of agronomically important traits.

Several studies provide valuable insights into the genetic basis of growth traits, such as DBH and total height, in various tree species. Rocha et al. [60] found significant associations in *Eucalyptus grandis* between DBH, TH, and volume measured in different years of data sampling, indicating a strong pleiotropic effect on trait associations. Cappa et al. [61] reported 16 single marker–trait associations for DBH in *Eucalyptus globulus*, suggesting that this trait is complex and influenced by multiple genes. Gion et al. [62] identified 4 QTLs

for growth in *Eucalyptus urophylla*, explaining between 4.1% and 11.9% of the phenotypic variation, while Freeman et al. [63] found 11 QTLs for growth in *Eucalyptus globulus*. In *Populus* spp., Du et al. [64] detected three QTLs for height, six for DBH, and eight for volume, which explained between 2.7% and 18.5% of the phenotypic variance. In contrast to our study, no genomic regions were identified that explained more than 1% of the total variation for the growth traits (TH and DBH). These traits exhibited typical polygenic behavior, where the entire genome contributed to their variation. This result confirms what has been reported in other studies, corroborating the complex architecture of growth traits and the pleiotropic effects among loci for growth traits [60,65]. Although multiple QTLs for these traits have been identified and reported in the literature, their effects tend to be small, highlighting the polygenic nature of these traits.

For ADFO, our study detected genomic regions that explained more than 1% of the total variation, but none exceeded 3%. Despite this, ADFO traits were found to be more heritable than growth traits. This could be because many SNPs have individual effects on the trait that are too small to be detected, but collectively they contribute to the total genetic variance observed [66–68], which highlights a typical polygenic behavior. Previous studies have associated the timing of the transition from juvenile to adult stages in *Eucalyptus globulus* populations with plant growth and environmental conditions [69], linking it to higher biotic pressure depending on environmental conditions, as well as plant mechanisms to minimize or escape damage [30,69–71].

In accordance with the genomic regions identified in this study that are associated with ADFO, the findings are consistent with previous research, which also highlighted chromosomes 3 and 11 as key regulators of disease resistance traits in *Eucalyptus* spp. [69,72–74]. These regions harbor genes that mediate resistance to biotic stresses, including defense responses to fungal infections [75,76]. For example, the *Glutathione transferase GST 23*, located on chromosome 11, plays a crucial role in detoxifying various toxic compounds, including fungal toxins [73]. Several studies have identified the microRNA *miR156* as the primary regulator of heteroblasty, controlling the expression of the *SQUAMOSA promoter binding protein-like* (SPL) transcription factor family [77–79]. These SPL proteins are involved in promoting the expression of adult traits, such as leaf development, vegetative phase change, and flower and fruit development [65,78–81]. However, some studies have reported that the expression of *miR156* may not be detected in certain contexts due to limitations in detection techniques, variability between species, or differences in experimental conditions [82,83]. This underscores the importance of considering the experimental context and methodology used. In this study, we were able to detect the primary genomic regions associated with heteroblasty on chromosomes 3 (positions 49,472,132 and 49,646,842 Mb) and 11 (positions 29,445,307 and 29,642,533 Mb).

5. Conclusions

This study enabled the estimation of genetic correlations and narrow-sense heritabilities for both disease and growth traits. It also demonstrated that the multi-trait threshold linear ssGWAS model effectively identified genomic regions associated with disease resistance traits, such as the proportion of adult foliage in the canopy, which serves as an escape mechanism against infection by *T. nubilosa*. These findings provide an opportunity for deeper exploration of these genomic regions to better understand the behavior of such traits. In contrast, growth traits (TH and DBH) exhibited typical polygenic behavior, with no genomic region explaining more than 1% of the total variation. Understanding the mechanisms underlying heteroblasty could enable forest genetic improvement programs to focus on identifying and selecting individuals that transition from juvenile to adult foliage at younger ages, thereby reducing their susceptibility to *T. nubilosa* infection.

Given the genetic correlations reported in this study, it is possible to select for ADFO at 21 months based on measurements taken at 14 months due to the strong genetic correlation between these traits. Selecting individuals with an early transition from juvenile to adult foliage presents an opportunity to enhance the sustainability and adaptation of *E. globulus* in environments where *T. nubilosa* is prevalent. Furthermore, these results could form the basis for developing and implementing genomic selection models to identify individuals with early foliage transition, supporting the long-term health and resilience of *E. globulus* plantations.

Author Contributions: Conceptualization, M.G., I.A., M.Q. and G.B.; methodology, M.G. and I.A.; formal analysis, M.G.; writing—original draft preparation, M.G.; writing—review and editing, I.A., M.Q. and G.B.; supervision, I.A. All authors have read and agreed to the published version of the manuscript.

Funding: The funding of this work came from INIA Uruguay (National Institute of Agricultural Research) and ANII (National Association of Investigation and Innovation Research).

Data Availability Statement: The data presented in this study are available on request from the corresponding author.

Acknowledgments: The authors thank INIA Uruguay and ANII for funding this work.

Conflicts of Interest: The authors declare no conflicts of interest.

References

1. Spindel, J.E.; Begum, H.; Akdemir, D.; Collard, B.; Redoña, E.; Jannink, J.-L.; McCouch, S. Genome-wide prediction models that incorporate de novo GWAS are a powerful new tool for tropical rice improvement. *Heredity* **2016**, *116*, 395–408. [CrossRef] [PubMed]
2. Tibbs, C.; Zhang, L.; Yu, J. Status and prospects of genome-wide association studies in plants. *Plant Genome* **2021**, *14*, e20077. [CrossRef]
3. Hirschhorn, J.N.; Daly, M.J. Genome-wide association studies for common diseases and complex traits. *Nat. Rev. Genet.* **2005**, *6*, 95–108. [CrossRef] [PubMed]
4. Hirschhorn, J.N.; Altshuler, D. The genetics of common diseases. *Nat. Rev. Genet.* **2002**, *3*, 247–258. [CrossRef]
5. Bolormaa, S.; Pryce, J.E.; Reverter, A.; Zhang, Y.; Barendse, W.; Kemper, K.; Goddard, M.E. A multi-trait, meta-analysis for detecting pleiotropic polymorphisms for stature, fatness and reproduction in beef cattle. *PLoS Genet.* **2014**, *10*, e1004198. [CrossRef] [PubMed]
6. Zhang, W.; Gao, X.; Shi, X.; Zhu, B.; Wang, Z.; Gao, H.; Chen, Y. PCA-based multiple-trait GWAS analysis: A powerful model for exploring pleiotropy. *Animals* **2018**, *8*, 239. [CrossRef] [PubMed]
7. Cappa, E.P.; Chen, C.; Klutsch, J.G.; Sebastian-Azcona, J.; Ratcliffe, B.; Wei, X.; El-Kassaby, Y.A. Multiple-trait analyses improved the accuracy of genomic prediction and the power of genome-wide association of productivity and climate change-adaptive traits in lodgepole pine. *BMC Genom.* **2022**, *23*, 536. [CrossRef] [PubMed]
8. Bolormaa, S.; Pryce, J.E.; Hayes, B.J.; Goddard, M.E. Multivariate analysis of a genome-wide association study in dairy cattle. *J. Dairy Sci.* **2010**, *93*, 3818–3833. [CrossRef] [PubMed]
9. Gualdrón Duarte, J.L.; Cantet, R.J.; Bates, R.O.; Ernst, C.W.; Raney, N.E.; Steibel, J.P. Rapid screening for phenotype-genotype associations by linear transformations of genomic evaluations. *BMC Bioinform.* **2014**, *15*, 246. [CrossRef]
10. Christensen, O.F.; Lund, M.S. Genomic prediction when some animals are not genotyped. *Genet. Sel. Evol.* **2010**, *42*, 2. [CrossRef]
11. Aguilar, I.; Misztal, I.; Johnson, D.; Legarra, A.; Tsuruta, S.; Lawlor, T. Hot topic: A unified approach to utilize phenotypic, full pedigree, and genomic information for genetic evaluation of Holstein final score1. *J. Dairy Sci.* **2010**, *93*, 743–752. [CrossRef]
12. Wang, M.; Cordell, H.; Van Steen, K. Statistical methods for genome-wide association studies. *Semin. Cancer Biol.* **2019**, *55*, 53–60. [CrossRef]
13. Wu, H.; Zhao, H. Efficient mixed-model association analysis for genome-wide association studies. *Nat. Methods* **2010**, *7*, 510–515. [CrossRef]
14. Hayes, B.; Goddard, M. Genome-wide association and genomic selection in animal breeding. *Genome* **2010**, *53*, 876–883. [CrossRef] [PubMed]
15. Legarra, A.; Ricard, A.; Varona, L. GWAS by GBLUP: Single and multimarker EMMAX and Bayes factors, with an example in detection of a major gene for horse gait. *G3 Genes Genomes Genet.* **2018**, *8*, 2301–2308. [CrossRef]

16. Habier, D.; Fernando, R.L.; Kizilkaya, K.; Garrick, D. Extension of the Bayesian alphabet for genomic selection. *BMC Bioinform.* **2011**, *12*, 186. [CrossRef] [PubMed]
17. Sun, X.; Habier, D.; Fernando, R.L.; Garrick, D.J.; Dekkers, J.C.M. Genomic breeding value prediction and QTL mapping of QTLMAS2010 data using Bayesian methods. *BMC Genet.* **2011**, *5*, S13. [CrossRef] [PubMed]
18. Peters, S.O.; Kizilkaya, K.; Garrick, D.J.; Fernando, R.L.; Reecy, J.M.; Weaber, R.L. Bayesian genome-wide association analysis of growth and yearling ultrasound measures of carcass traits in Brangus heifers. *J. Anim. Sci.* **2012**, *90*, 3398–3409. [CrossRef]
19. Goddard, M. Genomic selection: Prediction of accuracy and maximisation of long term response. *Genetica* **2009**, *136*, 245–257. [CrossRef] [PubMed]
20. Jurcic, E.J.; Villalba, P.V.; Pathauer, P.S.; Palazzini, D.A.; Oberschelp, G.P.; Harrand, L.; Cappa, E.P. Single-step genomic prediction of *Eucalyptus dunnii* using different identity-by-descent and identity-by-state relationship matrices. *Heredity* **2021**, *127*, 176–189. [CrossRef]
21. Bi, W.; Zhou, W.; Dey, R.; Mukherjee, B.; Sampson, J.N.; Lee, S. Efficient mixed model approach for large-scale genome-wide association studies of ordinal categorical phenotypes. *Am. J. Human. Genet.* **2021**, *108*, 825–839. [CrossRef]
22. Wright, S. An analysis of variability in number of digits in an inbred strain of guinea pigs. *Genetics* **1934**, *19*, 506–536. [CrossRef]
23. Gianola, D.; Foulley, J.L. Sire evaluation for ordered categorical data with a threshold model. *Genet. Sel. Evol.* **1983**, *15*, 201–224. [CrossRef] [PubMed]
24. Misztal, I.; Gianola, D.; Foulley, J.L. Computing aspects of a nonlinear method of sire evaluation for categorical data. *J. Dairy Sci.* **1989**, *72*, 1557–1568. [CrossRef]
25. Hunter, G.C.; Crous, P.W.; Carnegie, A.J.; Wingfield, M.J. *Teratosphaeria nubilosa*, a serious leaf disease pathogen of *Eucalyptus* spp. in native and introduced areas. *Mol. Plant Pathol.* **2009**, *10*, 1–14. [CrossRef] [PubMed]
26. Barber, P.A.; Carnegie, A.J.; Burgess, T.I.; Keane, P.J. Leaf diseases caused by *Mycosphaerella* species in *Eucalyptus globulus* plantations and nearby native forest in the Green Triangle Region of southern Australia. *Australas. Plant Pathol.* **2008**, *37*, 472–481. [CrossRef]
27. Smith, A.H.; Potts, B.M.; Ratkowsky, D.A.; Pinkard, E.A.; Mohammed, C.L. Association of *Eucalyptus globulus* leaf anatomy with susceptibility to *Teratosphaeria* leaf disease. *For. Pathol.* **2018**, *48*, e12395. [CrossRef]
28. Dungey, H.S.; Potts, B.M.; Carnegie, A.J.; Ades, P.K. *Mycosphaerella* leaf disease: Genetic variation in damage to *Eucalyptus nitens*, *Eucalyptus globulus*, and their F1 hybrid. *Can. J. For. Res.* **1997**, *27*, 750–759. [CrossRef]
29. Potts, B.; Milgate, A.W.; Joyce, K.; Mohammed, C.L.; Vaillancourt, R.; Dutkowski, G.W. Quantitative genetic control of Mycosphaerella resistance in *Eucalyptus globulus* and impact on growth. University of Tasmania. In Proceedings of the Eucalyptus in a Changing World. IUFRO Conference, Aveiro, Portugal, 11–15 October 2004. Available online: https://hdl.handle.net/102.100.100/493193 (accessed on 27 December 2024).
30. Milgate, A.W.; Potts, B.M.; Joyce, K.; Mohammed, C.; Vaillancourt, R.E. Genetic variation in *Eucalyptus globulus* for susceptibility to *Mycosphaerella nubilosa* and its association with tree growth. *Australas. Plant Pathol.* **2005**, *34*, 11–18. [CrossRef]
31. James, S.A.; Bell, D.T. Leaf morphological and anatomical charac-teristics of heteroblastic *Eucalyptus globulus* ssp. *globulus* (Myrtaceae). *Aust. J. Bot.* **2001**, *49*, 259–269. [CrossRef]
32. Hamilton, M.G.; Tilyard, P.A.; Williams, D.R.; Vaillancourt, R.E.; Wardlaw, T.J.; Potts, B.M. Genetic variation in the timing of hetero- blastic transition in *Eucalyptus globulus* is stable across environments. *Aust. J. Bot.* **2011**, *59*, 170–175. [CrossRef]
33. Quezada, M.; Giorello, F.M.; Da Silva, C.C.; Aguilar, I.; Balmelli, G. Single-step genome-wide association study for susceptibility to *Teratosphaeria nubilosa* and precocity of vegetative phase change in *Eucalyptus globulus*. *Front. Plant Sci.* **2023**, *14*, 1124768. [CrossRef]
34. Silva-Junior, O.B.; Faria, D.A.; Grattapaglia, D. A flexible multi-species genome-wide 60K SNP chip developed from pooled resequencing of 240 *Eucalyptus* tree genomes across 12 species. *New Phytol.* **2015**, *206*, 1527–1540. [CrossRef]
35. Aguilar, I.; Tsuruta, S.; Masuda, Y.; Lourenco, D.A.L.; Legarra, A.; Misztal, I. BLUPF90 suite of programs for animal breeding with focus on genomics. In Proceedings of the World Congress on Genetics Applied to Livestock Production, Auckland, Australia, 13 February 2018. Available online: https://nce.ads.uga.edu/wiki/doku.php?id=start (accessed on 6 October 2023).
36. Misztal, I.; Tsuruta, S.; Strabel, T.; Auvray, B.; Druet, T.; Lee, D. BLUPF90 and related programs (BGF90). In Proceedings of the 7th World Congress on Genetics Applied to Livestock Production, CD-ROM Communication, Montpellier, France, 19–23 August 2002. Available online: https://nce.ads.uga.edu/wiki/doku.php?id=start (accessed on 6 October 2023).
37. Yin, L.; Zhang, H.; Tang, Z.; Xu, J.; Yin, D.; Zhang, Z.; Yuan, X.; Zhu, M.; Zhao, S.; Li, X.; et al. rMVP: A Memory-efficient, Visualization-enhanced, and Parallel-accelerated Tool for Genome-wide Association Study. *Genom. Proteom. Bioinform.* **2021**, *19*, 619–628. [CrossRef]
38. Wickham, H. *ggplot2: Elegant Graphics for Data Analysis*; Springer: Berlin/Heidelberg, Germany, 2016.
39. R Core Team. *R: A Language and Environment for Statistical Computing*; R Foundation for Statistical Computing: Vienna, Austria, 2023. Available online: https://www.R-project.org/ (accessed on 2 March 2023).

40. Legarra, A.; Aguilar, I.; Misztal, I. A relationship matrix including full pedigree and genomic information. *J. Dairy Sci.* **2009**, *92*, 4656–4663. [CrossRef] [PubMed]
41. Strandén, I.; Garrick, D.J. Technical note: Derivation of equivalent computing algorithms for genomic predictions and reliabilities of animal merit. *J. Dairy Sci.* **2009**, *92*, 2971–2975. [CrossRef] [PubMed]
42. VanRaden, P. Efficient methods to compute genomic predictions. *J. Dairy Sci.* **2008**, *91*, 4414–4423. [CrossRef]
43. Tsuruta, S.; Misztal, I. THRGIBBSF90 for estimation of variance components with threshold and linear models. In Proceedings of the 8th World Congress Genetics Applied to Livestock Production, CD-ROM Communication, Belo Horizonte, Brazil, 13–18 August 2006.
44. Aguilar, I.; Misztal, I.; Tsuruta, S.; Legarra, A.; Wang, H. PREGSF90—POSTGSF90: Computational tools for the implementation of single-step genomic selection and genome-wide association with ungenotyped individuals in BLUPF90 programs. In Proceedings of the 10th World Congress on Genetics Applied to Livestock Production, Vancouver, BC, Canada, 17–22 August 2014.
45. Carnegie, A.J.; Ades, P.K. Mycosphaerella leaf disease reduces growth of plantation-grown *Eucalyptus globulus*. *Aust. For.* **2003**, *66*, 113–119. [CrossRef]
46. Grattapaglia, D.; Kirst, M. *Eucalyptus* applied genomics: From gene sequences to breeding tools. *New Phytol.* **2008**, *179*, 911–929. [CrossRef] [PubMed]
47. Zhu, L.; Ni, W.; Liu, S.; Cai, B.; Xing, H.; Wang, S. Transcriptomics Analysis of Apple Leaves in Response to *Alternaria alternata* Apple Pathotype Infection. *Front. Plant Sci.* **2017**, *8*, 22. [CrossRef] [PubMed]
48. Vlasveld, C.; O'Leary, B.; Udovicic, F.; Burd, M. Leaf heteroblasty in eucalypts: Biogeographic evidence of ecological function. *Aust. J. Bot.* **2018**, *66*, 191–201. [CrossRef]
49. Begum, H.; Spindel, J.E.; Lalusin, A.; Borromeo, T.; Gregorio, G.; Hernandez, J.; Virk, P.; Collard, B.; McCouch, S.R. Genome-wide association mapping for yield and other agronomic traits in an elite breeding population of tropical rice (*Oryza sativa*). *PLoS ONE* **2015**, *10*, e0119873. [CrossRef] [PubMed]
50. Resende, R.T.; Resende, M.D.V.; Silva, F.F.; Azevedo, C.F.; Takahashi, E.K.; Silva-Junior, O.B.; Grattapaglia, D. Regional heritability mapping and genome-wide association identify loci for complex growth, wood and disease resistance traits in *Eucalyptus*. *New Phytol.* **2017**, *213*, 1287–1300. [CrossRef]
51. Klápště, J.; Ismael, A.; Paget, M.; Graham, N.J.; Stovold, G.T.; Dungey, H.S.; Slavov, G.T. Genomics-enabled management of genetic resources in radiata pine. *Forests* **2022**, *13*, 282. [CrossRef]
52. Costa e Silva, J.; Potts, B.M.; Tilyard, P. Stability of genetic effects across clonal and seedling populations of *Eucalyptus globulus* with common parentage. *For. Ecol. Manag.* **2013**, *291*, 427–435. [CrossRef]
53. Hamilton, M.G.; Williams, D.R.; Tilyard, P.A.; Pinkard, E.A.; Wardlaw, T.J.; Glen, M.; Vaillancourt, R.E.; Potts, B.M. A latitudinal cline in disease resistance of a host tree. *Heredity* **2013**, *110*, 372–379. [CrossRef]
54. Volker, P.W.; Potts, B.M.; Borralho, N.M.G. Genetic parameters of intra- and inter-specific hybrids of *Eucalyptus globulus* and *E. nitens*. *Tree Genet. Genomes* **2008**, *4*, 445–460. [CrossRef]
55. Marco de Lima, B.; Cappa, E.P.; Silva-Junior, O.B.; Garcia, C.; Mansfield, S.D.; Grattapaglia, D. Quantitative genetic parameters for growth and wood properties in *Eucalyptus* "urograndis" hybrid using near-infrared phenotyping and genome-wide SNP-based relationships. *PLoS ONE* **2019**, *14*, e0218747. [CrossRef]
56. Haristoy, G.; Bouffier, L.; Fontes, L.; Leal, L.; Paiva, J.A.; Pina, J.P.; Gion, J.M. Genomic prediction in a multi-generation *Eucalyptus globulus* breeding population. *Tree Genet. Genomes* **2023**, *19*, 8. [CrossRef]
57. Fernando, R.; Toosi, A.; Wolc, A.; Garrick, D.; Dekkers, J. Application of whole-genome prediction methods for genome-wide association studies: A Bayesian approach. *J. Agric. Biol. Environ. Stat.* **2017**, *22*, 172–193. [CrossRef]
58. Porter, H.F.; O'Reilly, P.F. Multivariate simulation framework reveals performance of multi-trait GWAS methods. *Sci. Rep.* **2017**, *7*, srep38837. [CrossRef]
59. Fernandes, S.B.; Casstevens, T.M.; Bradbury, P.J.; Lipka, A.E. A multi-trait multi-locus stepwise approach for conducting GWAS on correlated traits. *Plant Genome* **2022**, *15*, e20200. [CrossRef]
60. Rocha, L.F.; Benatti, T.R.; de Siqueira, L.; de Souza, I.C.G.; Bianchin, I.; de Souza, A.J.; Tambarussi, E.V. Quantitative trait loci related to growth and wood quality traits in *Eucalyptus grandis W. Hill* identified through single- and multi-trait genome-wide association studies. *Tree Genet. Genomes* **2022**, *18*, 38. [CrossRef]
61. Cappa, E.P.; El-Kassaby, Y.A.; Garcia, M.N.; Acuña, C.; Borralho, N.M.G.; Grattapaglia, D.; Poltri, S. Impacts of Population Structure and Analytical Models in Genome-Wide Association Studies of Complex Traits in Forest Trees: A Case Study in *Eucalyptus globulus*. *PLoS ONE* **2013**, *8*, e81267. [CrossRef] [PubMed]
62. Gion, J.M.; Carouché, A.; Deweer, S.; Bedon, F.; Pichavant, F.; Charpentier, J.P.; Baillères, H.; Rozenberg, P.; Carocha, V.; Ognouabi, N.; et al. Comprehensive genetic dissection of wood properties in a widely-grown tropical tree: *Eucalyptus*. *BMC Genom.* **2011**, *12*, 301. [CrossRef]

63. Freeman, J.S.; Potts, B.M.; Downes, G.M.; Pilbeam, D.; Thavamanikumar, S.; Vaillancourt, R.E. Stability of quantitative trait loci for growth and wood properties across multiple pedigrees and environments in *Eucalyptus globulus*. *New Phytol.* **2013**, *198*, 1121–1134. [CrossRef] [PubMed]
64. Du, Q.; Gong, C.; Wang, Q.; Zhou, D.; Yang, H.; Pan, W.; Li, B.; Zhang, D. Genetic architecture of growth traits in Populus revealed by integrated quantitative trait locus (QTL) analysis and association studies. *New Phytol.* **2016**, *209*, 1067–1082. [CrossRef] [PubMed]
65. Muller, B.S.; de Almeida Filho, J.E.; Lima, B.M.; Garcia, C.C.; Missiaggia, A.; Aguiar, A.M. Independent and joint-GWAS for growth traits in *Eucalyptus* by assembling genome-wide data for 3373 individuals across four breeding populations. *New Phytol.* **2019**, *221*, 818–833. [CrossRef] [PubMed]
66. Yang, J.; Benyamin, B.; McEvoy, B.P.; Gordon, S.; Henders, A.K.; Nyholt, D.R.; Madden, P.A.; Heath, A.C.; Martin, N.G.; Montgomery, G.W.; et al. Common SNPs explain a large proportion of the heritability for human height. *Nat. Genet.* **2010**, *42*, 565–569. [CrossRef] [PubMed]
67. Peiffer, J.A.; Romay, M.C.; Gore, M.A.; Flint-Garcia, S.A.; Zhang, Z.; Millard, M.J.; Gardner, C.A.; McMullen, M.D.; Holland, J.B.; Bradbury, P.J.; et al. The genetic architecture of maize height. *Genetics* **2014**, *196*, 1337–1356. [CrossRef]
68. Brookfield, J.F. Quantitative genetics: Heritability is not always missing. *Curr. Biol.* **2013**, *23*, R276–R278. [CrossRef]
69. Jordan, G.J.; Potts, B.M.; Chalmers, P.; Wiltshire, R.J. Quantitative genetic evidence that the timing of vegetative phase change in *Eucalyptus globulus* ssp. globulus is an adaptive trait. *Aust. J. Bot.* **2000**, *48*, 561–567. [CrossRef]
70. Brawner, J.T.; Lee, D.J.; Hardner, C.M. Relationships between early growth and *Quambalaria* shoot blight tolerance in *Corymbia citriodora* progeny trials established in Queensland, Australia. *Tree Genet. Genomes* **2011**, *7*, 759–772. [CrossRef]
71. Bonora, F.; Hayes, R.A.; Nahrung, H.F.; Lee, D.J. Spotted gums and hybrids: Impact of pests and diseases, ontogeny and climate on tree performance. *For. Ecol. Manag.* **2020**, *472*, 118235. [CrossRef]
72. Dielen, A.S.; Badaoui, S.; Candresse, T.; German-Retana, S. The ubiquitin/26s proteasome system in plant–pathogen interactions: A never-ending hide-and-seek game. *Mol. Plant Pathol.* **2010**, *11*, 293–308. [CrossRef]
73. Gardiner, S.A.; Boddu, J.; Berthiller, F.; Hametner, C.; Stupar, R.M.; Adam, G. Transcriptome analysis of the barley–deoxynivalenol interaction: Evidence for a role of glutathione in deoxynivalenol detoxification. *Mol. Plant-Microbe Interact.* **2010**, *23*, 962–976. [CrossRef]
74. Yadav, V.; Wang, Z.; Yang, X.; Wei, C.; Changqing, X.; Zhang, X. Comparative analysis, characterization and evolutionary study of dirigent gene family in cucurbitaceae and expression of novel dirigent peptide against powdery mildew stress. *Genes* **2021**, *12*, 326. [CrossRef]
75. Nagpure, A.; Choudhary, B.; Gupta, R.K. Chitinases: In agriculture and human healthcare. *Crit. Rev. Biotechnol.* **2014**, *34*, 215–232. [CrossRef] [PubMed]
76. Rodrıǵuez, A.; Shimada, T.; Cervera, M.; Alquézar, B.; Gadea, J.; Gómez-Cadenas, A. Terpene down-regulation triggers defense responses in transgenic orange leading to resistance against fungal pathogens. *Plant Physiol.* **2014**, *164*, 321–339. [CrossRef]
77. Poethig, R.S. The past, present, and future of vegetative phase change. *Plant Physiol.* **2010**, *154*, 541–544. [CrossRef] [PubMed]
78. Hudson, C.J.; Freeman, J.S.; Jones, R.C.; Potts, B.M.; Wong, M.M.; Weller, J.L. Genetic control of heterochrony in *Eucalyptus globulus*. *G3 Genes Genomes Genet.* **2014**, *4*, 1235–1245. [CrossRef]
79. Manuela, D.; Xu, M. Juvenile leaves or adult leaves: Determinants for vegetative phase change in flowering plants. *Int. J. Mol. Sci.* **2020**, *21*, 9753. [CrossRef] [PubMed]
80. Yang, L.; Xu, M.; Koo, Y.; He, J.; Poethig, R.S. Sugar promotes vegetative phase change in *Arabidopsis thaliana* by repressing the expression of MIR156A and MIR156C. *eLife* **2013**, *2*, e00260. [CrossRef]
81. Rubio-Somoza, I.; Zhou, C.M.; Confraria, A.; Martinho, C.; von Born, P.; Baena-Gonzalez, E.; Wang, J.W.; Weigel, D. Temporal control of leaf complexity by miRNA-Regulated licensing of protein complexes. *Curr. Biol.* **2014**, *24*, 2714–2719. [CrossRef] [PubMed]
82. Wu, G.; Park, M.Y.; Conway, S.R.; Wang, J.W.; Weigel, D.; Poethig, R.S. The sequential action of miR156 and miR172 regulates developmental timing in Arabidopsis. *Cell* **2009**, *138*, 750–759. [CrossRef] [PubMed]
83. Liu, Q.; Wang, F.; Axtell, M.J. Analysis of complementarity requirements for plant microRNA targeting using a *Nicotiana benthamiana* quantitative transient assay. *Plant Cell* **2014**, *26*, 741–753. [CrossRef] [PubMed]